Experimental Investigation of the Effect of Random Packings on Heat Transfer and Particle Segregation in Packed-Fluidized Bed

I&EC research
Industrial & Engineering Chemistry Research
pubs.acs.org/IECR
Article

Experimental Investigation of the Effect of Random Packings on Heat Transfer and Particle Segregation in Packed-Fluidized Bed

Nasrin Nemati,* Pontus Andersson, Viktor Stenberg, and Magnus Rydén

Cite This: *Ind. Eng. Chem. Res.* 2021, 60, 10365−10375
Read Online
ACCESS | Metrics & More | Article Recommendations

ABSTRACT: The heat transfer coefficient, pressure drop, and vertical segregation in a bubbling fluidized bed reactor containing random packings were investigated. The bed material was silica sand in the size range of 90−400 μm. Experiments were done for bed temperatures ranging from 400 to 900 °C and superficial gas velocities up to 0.411 m/s. Five different types of packings were evaluated: (i) RMSR (25 mm stainless steel thread saddle ring), (ii) Hiflow (25 mm stainless steel pall ring), (iii) RR6 (6 mm ceramic Raschig ring), (iv) RR10 (10 mm ceramic Raschig ring), and (v) ASB (12.7 mm aluminum silicate balls). The RMSR packing showed an increase in the heat transfer coefficient (up to 1243 W/m^{2}K), as compared to bubbling beds with no packings (up to 1124 W/m^{2}K). Also, beds with RMSR and Hiflow packings had a lower pressure drop and vertical segregation compared to low void factor packings such as RR6, RR10, and ASB.

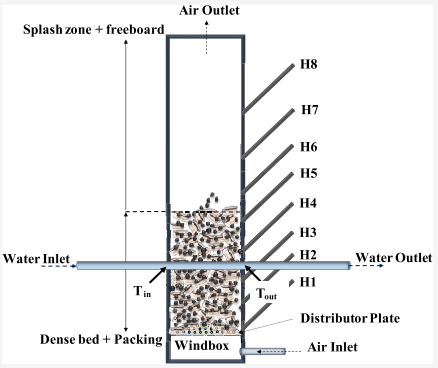

1. INTRODUCTION

Fluidization was established as an industrially important concept in the 1940s, during which large-scale implementation of fluid catalytic cracking was widely introduced. It soon extended its range of applications to other areas such as heat transfer, coatings, drying, combustion, gasification, chemical reactors, and adsorption.[1−4] One of the advantages of fluidized beds is their ability to provide a relatively uniform bed temperature and high rates of heat transfer.[5] Therefore, they can be used as heat exchanger apparatuses with good performance. In a fluidized bed heat exchanger, tubes are immersed in the dense zone of a fluidized bed and heat transfer will occur between the bed particles and the tube wall.[6] Significant research has been conducted to study the phenomena experimentally, as well as present predictive expressions for the bed-to-tube heat transfer rate in different fluidization regimes.[7−12]

In bubbling fluidized bed heat exchangers, the heat transfer rate is determined by solid particles in motion that come in contact with the immersed tubes, as well as the bubble size.[6,13] Geldart divided different particulate materials into four main groups based on their density, diameter, different flow regimes, and fluidization characteristics.[14,15] Among these groups, Geldart group B with bulk density in the range of 1400−4000 kg/m^3 and diameter of 40−500 μm has proven to be very useful in industrial applications.[16−18] However, fluidization of Geldart B particles has its own challenges such as bubble coalescence and bubble growth. This can result in phenomena such as slugging and channeling, especially at high temperatures and high gas velocities. This in turn may result in negative effects, e.g., a reduced rate of heat transfer.[19−22]

Various methods for overcoming this restriction and improving the quality of gas−solid fluidization have been proposed. The methods range from adding mechanical constructs, such as disks, trays, and concentric mesh screens, to adding movable packings, such as glass beads, berl saddles, and Raschig rings. The purpose of such devices is to break down the large bubbles formed inside the bed into smaller ones.[13,23] The use of fixed parts involves certain problems, such as erosion, difficulties in replacing worn-out parts, and potential mechanical stress for operation at elevated temperatures. As for packed-fluidized beds, the few studies that exist are focused on a few packing types, especially spherical packings with a low void factor. Donsi et al.[24,25] and Girimonte et al.[26,27] studied the expansion behavior of fine particles in a packed bed of spherical coarse particles at room temperature, in the velocity range up to 10 times the minimum fluidization velocity. Both research groups presented models for the bed expansion behavior of particles in a packed-fluidized bed, based on experimental results. The models describe hydrodynamic properties such as pressure drop, minimum fluidization velocity, and bed voidage. In other works, Girimonte et

Received: March 29, 2021
Revised: June 15, 2021
Accepted: June 16, 2021
Published: July 12, 2021

https://doi.org/10.1021/acs.iecr.1c01221
Ind. Eng. Chem. Res. 2021, 60, 10365−10375

al.[28,29] investigated CO_2 adsorption on zeolite pellets in a packed-fluidized bed using glass spheres as packings. They observed that for a given mass of sorbents, CO_2 adsorption increased compared to fixed beds because of suppression of bubble growth. Mandal et al.[30−34] performed a wide range of experiments on the hydrodynamics of packed-fluidized beds with spherical packings. They investigated minimum fluidization velocity, void fraction, and effective thermal conductivity in these systems and proposed empirical models to predict the behavior of beds containing spherical packings, including minimum fluidization velocity. In another work[35] Mandal et al. investigated the quality of fluidization in packed-fluidized beds by γ ray transmission technique. They concluded that for beds containing spherical packings, fluidization would be more homogeneous compared to beds with no packing.

The use of random packings in a fluidized bed would break down bubbles and prevent bubble growth, but it could also constitute a major hindrance for fluidization. It may also influence factors such as the heat transfer rate significantly compared to nonpacked beds.[13] Studies on fluidized-packed beds with evolved packing materials and the impact on factors such as heat transfer rate and particle segregation are currently lacking.

1.1. Aim of This Study. The aim of this study is to examine packed-fluidized beds with five different random packings and their effect on heat transfer, pressure drop, and particle segregation. Two highly evolved packings with very high void factors have been included among the five packings chosen.

2. EXPERIMENTAL SECTION

2.1. Bed Material and Packings. The bed material used in all experiments was silica sand supplied by Sibelco Nordic AB. It was sieved to the size range of 90−400 μm. Using sieves for particle sizes 90, 180, 212, 250, 300, and 355 μm, the weighted mean particle diameter for the used interval was calculated to be 240 μm. The particle size distribution is provided in Figure 1.

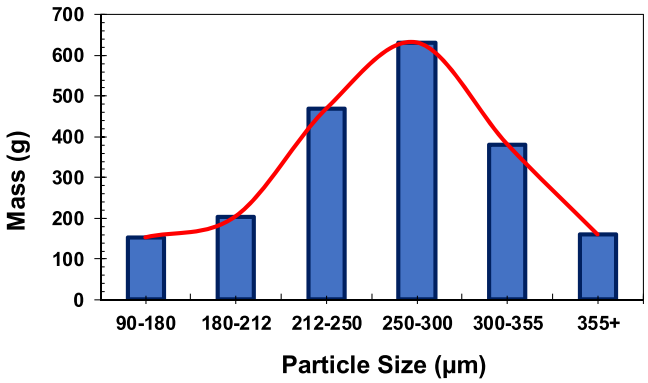

Figure 1. Particle size distribution for the silica sand used.

The bulk density of the bed material was 1594 kg/m^3. It was calculated by pouring sand particles into a container with a known volume, recording the change in mass, and dividing it by the volume. The sphericity of the sand particles was assumed to be 0.67, which is a typical value for sharp sands according to Daizo and Levenspiel.[1] The minimum fluidization velocity of particles in a bed with no packing was calculated with eq 1, as proposed by Chitester et al.[1] The minimum fluidization velocity for sand particles at 400 °C was calculated to be 0.04 m/s. The corresponding value at 900 °C was 0.03 m/s. As the bed temperature increases, the minimum fluidization velocity decreases as a result of decreasing fluidizing gas density and its increasing viscosity. For packed-fluidized beds, similar tendencies can be expected. Although no studies are available for evolved packing materials, Kulkarni et al.[36] and Mandal et al.[30] have investigated the minimum fluidization velocity in packed-fluidized beds for spherical packings.

$$\frac{d_p u_{mf} \rho_g}{\mu} = \left[(28.7)^2 + 0.0494 \left(\frac{d_p^3 \rho_g (\rho_s - \rho_g) g}{\mu^2} \right) \right]^{1/2} - 28.7 \quad (1)$$

Five different types of packings were examined: (i) 12.7 mm aluminum silicate balls (ASB), (ii) 10 mm ceramic Raschig rings (RR10), (iii) 6 mm ceramic Raschig rings (RR6), (iv) 25 mm stainless steel thread saddle rings RMSR 25-3 (RMSR), and (v) 25 mm stainless steel pall rings Hiflow 25-5 (Hiflow). Pictures of the packings are shown in Figure 2.

The bulk density of the packings was measured by the same principle as outlined for the bed material. The void factor of the packings was determined by adding packings to a known volume and measuring how much water was needed to fill the container entirely. The volume of water corresponds to the void in the packed bed, which allowed for the calculation of the void factor. In all experiments, the unfluidized bed height was about 13 cm. This was to assure that the horizontal water tube is totally covered with the bed material. Also, using a fixed bed height, pressure measurements could be used to evaluate solid segregation, as will be discussed below. The required mass of packings and silica sand for each measuring campaign was estimated by filling a container with a similar size of reactor up to 13 cm height and then measuring its weight changes. Table 1 provides packing and bed material information for each set of experiments.

2.2. Experimental Setup. The experiments were conducted in a cylindrical laboratory-scale bubbling fluidized bed reactor made of 253 MA steel, with an inner diameter of 77.9 mm and a height of 1.27 m. The fluidization gas was dry air, which was fed to the reactor by a mass flow controller via a windbox. A gas distribution plate was located at the top of the windbox. It was in the form of a hole plate with 5 mm thickness and 61 circular holes of 0.6 mm diameter each. Since the holes in the hole plate were larger than the particles, a small gas flow was applied also during the down time to prevent the particles from falling into the windbox. The heat needed to reach the desired bed temperature was provided by an electric furnace enclosing the reactor. Since the windbox was located inside the furnace, the fluidization gas was preheated essentially to the bed temperature before it enters the reactor. The hot gas exiting the reactor was collected by a ventilation hood located above the reactor exit.

A single horizontal tube made of Inconel 600 alloy with an inner diameter of 4 mm and a thickness of 1 mm was positioned 75 mm above the gas distributor plate. Water flowed through the horizontal tube from a tap. The flow rate was regulated with a valve. During all experiments, the water flow rate through the pipe used for measuring the heat transfer coefficient was kept constant at 20 mL/s. In previous

https://doi.org/10.1021/acs.iecr.1c01221
Ind. Eng. Chem. Res. 2021, 60, 10365−10375

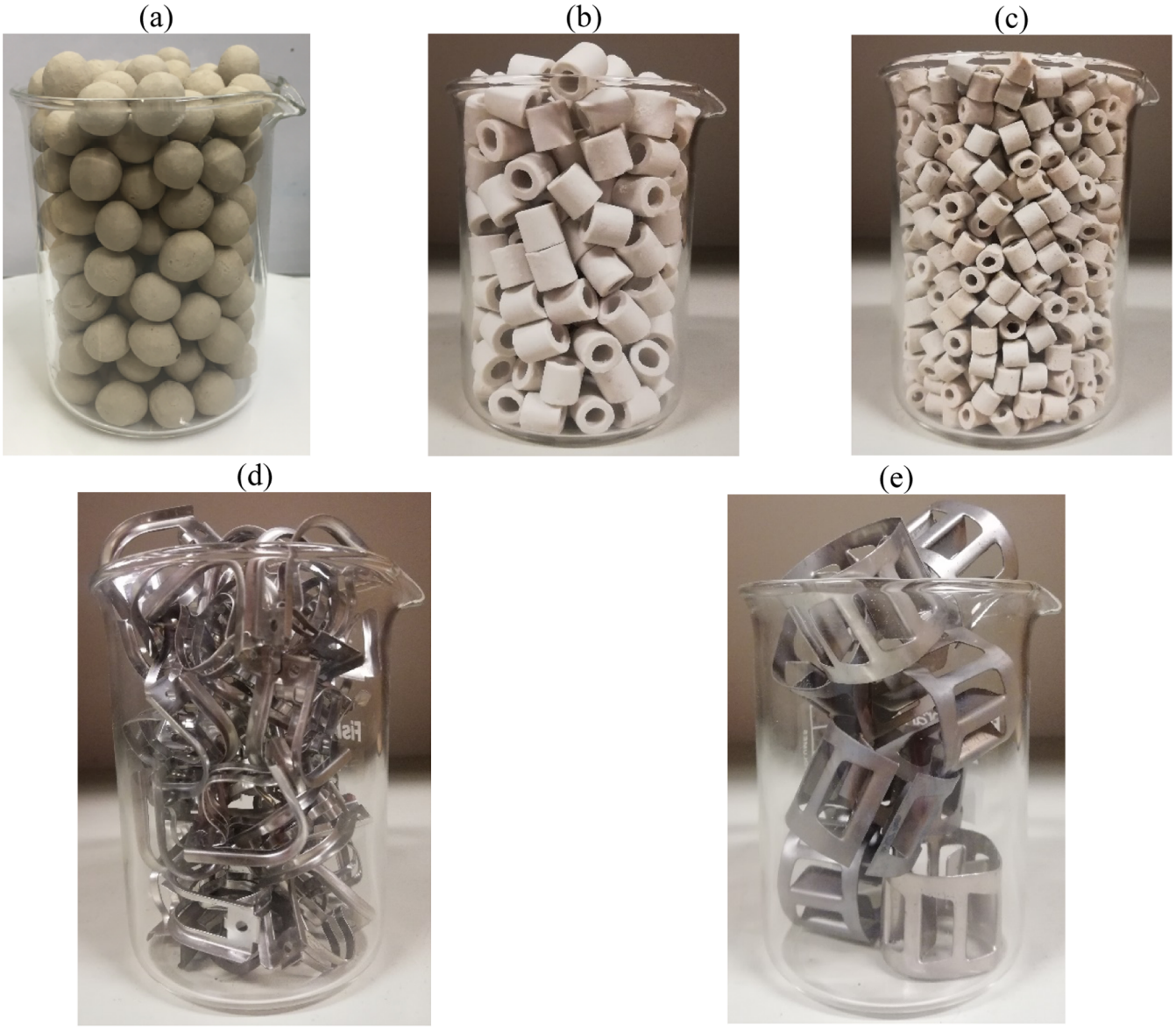

Figure 2. Packings evaluated in this study: (a) ASB (12.7 mm), (b) RR10 (10 mm), (c) RR6 (6 mm), (d) RMSR (25 mm), and (e) Hiflow (25 mm).

Table 1. Description of Experimental Parameters, with a Bed Containing No Packing as a Reference Case[a]

packing	void factor of packing (−)	bulk density of packing (kg/m^3)	mass of packing (g)	mass of silica sand (g)
ASB	0.43	1390	872.7	438.2
RR6	0.50	1110	686.1	559.0
RR10	0.58	890	586.7	619.1
RMSR	0.96	204	133.6	967.8
Hiflow	0.95	280	162.3	931.8
unpacked bed	1	0	0.0	988.1

[a]All beds had a nominal bed height of 13 cm at rest.

experiments using the same general reactor setup, the flow has been verified to be in the turbulent regime and sufficiently high to prevent boiling inside the tube.[37] The water was collected and weighed on a scale after exiting the reactor to ensure accurate determination of the flow rate. The temperatures of the flow at the inlet and outlet were measured with thermocouples. A schematic illustration of the experimental setup is shown in Figure 3.

Several pipes, inclined at 45°, were connected to the reactor, allowing for pressure and temperature sensors. Table 2 indicates the vertical positions of measurement points. Pressure transducers were placed in positions 2, 5, 7, 8, and windbox. Thermocouples were placed in the positions of 1, 3, 4, 6, and windbox. Each thermocouple was inserted 10 mm inside the bed, with an inclined angle of 45°.

2.3. Methodology. During experiments, the bed temperature was varied in the range of 400−900 °C, and the superficial gas velocity in the range of 0.04−0.411 m/s. When examining the impact of temperature, the superficial gas velocity was set to 0.2 m/s. When examining the impact of superficial gas velocity, the temperature was set to 800 °C. For each set of experimental parameters, data was gathered at a steady state over a period of 60 s, during which pressure and temperature data were recorded once every second. The water

https://doi.org/10.1021/acs.iecr.1c01221
Ind. Eng. Chem. Res. 2021, 60, 10365−10375

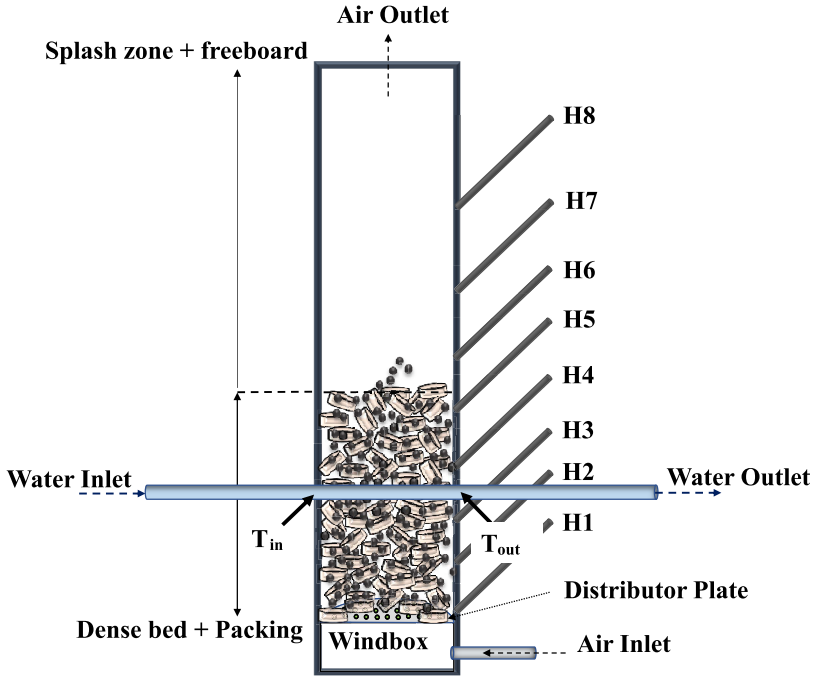

Figure 3. Schematic illustration of the experimental setup and apparatus.

Table 2. Vertical Position of Measurement Points Relative to the Distributor Plate

position	height (mm)	measured data
windbox		temperature and pressure
1	30	temperature
2	47	pressure
3	65	temperature
water tube	75	temperature
4	105	temperature
5	130	pressure
6	150	temperature
7	310	pressure
8	605	pressure

flow rate was verified by gathering 60 s worth of flow, weighing it on a scale, and dividing it with the density of water at the average water temperature. For all practical purposes, the bed temperature could be regarded as constant over the 60 s periods. For data analysis, the bed temperature data measured in position 1 at 30 mm above the distributor plate was used.

3. DATA EVALUATION

3.1. Bed-to-Tube Heat Transfer Coefficient. Figure 4 shows a general overview of thermal resistances for heat transfer from the fluidized bed to the water flowing inside the tube. Measuring the inlet and outlet water temperatures, water flow rate, and bed temperature will enable a calculation of the average bed-to-tube heat transfer coefficient.

Bed-to-tube heat transfer coefficient, h_o, was calculated by applying the overall heat transfer coefficient formula through a tube[38,39]

$$h_o = \frac{1}{\frac{1}{U_o} - \frac{d_o \ln(d_o/d_i)}{2k_{wall}} - \frac{d_o}{d_i h_i}} \tag{2}$$

where, k_{wall} is the thermal conductivity of the tube wall, which was estimated from material data for the average temperature

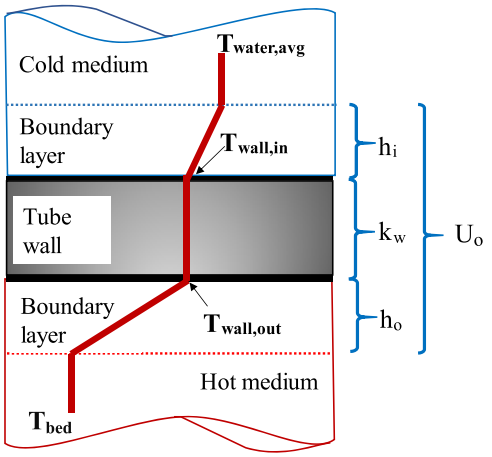

Figure 4. Thermal resistances for heat transfer from fluidized bed to water flow inside the tube.

of the tube wall. In the above equation, U_o is the overall heat transfer coefficient and can be determined as presented below (see eqs 3−6)[38,39]

$$U_o = \frac{Q}{A_o \Delta T_{LM}} \tag{3}$$

$$\Delta T_{LM} = \frac{\Delta T_{in} - \Delta T_{out}}{\ln(\Delta T_{in}/\Delta T_{out})} \tag{4}$$

$$\Delta T_{in} = T_{bed} - T_{water,inlet} \tag{5}$$

$$\Delta T_{out} = T_{bed} - T_{water,outlet} \tag{6}$$

where the temperature of the packed-fluidized bed, T_{bed}, and heat transfer rate between the bed and water flow, Q, are assumed to be constant along the whole tube length. Q can be calculated as[38,39]

https://doi.org/10.1021/acs.iecr.1c01221
Ind. Eng. Chem. Res. 2021, 60, 10365−10375

$$Q = \rho_{water} \dot{V} c_{p,water} (T_{water,outlet} - T_{water,inlet}) \quad (7)$$

where, water density, ρ_{water}, and its heat capacity, $c_{p,water}$, were taken at the average water temperature.

Stenberg et al.[37] used the average value calculated by correlations for turbulent flow to predict the h_i coefficient. The case with water flowing in a pipe is straightforward and empirical expressions could be expected to provide good accuracy. All expressions examined also provided very similar estimations for h_i (eqs 8−10)[40]

$$h_i = 0.023 \frac{k_{water}}{d_i} Re^{0.8} Pr^{0.4} \quad (8)$$

$$h_i = \frac{k_{water}}{d_i} j_h RePr^{0.33} \quad (9)$$

$$h_i = \frac{4200(1.35 + 0.02T_{water,avg}) u_{water}^{0.8}}{d_i^{0.2}} \quad (10)$$

In the above equations, k_{water} is the thermal conductivity of water, u_{water} is the average velocity of water flowing through the horizontal tube, and j_h is the heat transfer factor for the inside of the horizontal tube.

As mentioned above, k_{wall} was estimated at the average temperature of the tube wall. For this purpose, the temperature of the inner side of the tube, $T_{wall,in}$, was obtained using the tube-to-water heat transfer coefficient, h_i, as follows

$$T_{wall,in} = \frac{Q}{h_i A_i} + T_{water,avg} \quad (11)$$

Heat transferred through the tube wall was used to determine the temperature on the outer side of the tube, $T_{wall,out}$, by eq 14. However, the thermal conductivity used in this equation is in turn dependent on the outer tube wall temperature. A solution is obtained iteratively by initially guessing $T_{wall,out}$ (eqs 12−14).

$$k_{wall} = f(T_{wall,avg}) \quad (12)$$

$$T_{wall,avg} = \frac{T_{wall,out} + T_{wall,in}}{2} \quad (13)$$

$$Q = \frac{2k_{wall}}{d_o \ln(d_o/d_i)} A_o (T_{wall,out} - T_{wall,in}) \quad (14)$$

3.2. Pressure Drop Across Packed-Fluidized Bed. As explained by Sutherland et al.[13] and Daizo and Levenspiel,[1] when fluidization occurs in a particulate bed, the pressure drop becomes equal to the effective weight of the bed and can be calculated as

$$\Delta P_{bed} = H(1 - \varepsilon_{bed})(\rho_s - \rho_g) \frac{g}{g_c} \quad (15)$$

In principle, after reaching the minimum fluidization velocity, the pressure drop will become constant. Thus, there will be a sharp discontinuity of the pressure drop plot as a function of superficial gas velocity. However, defining the minimum fluidization point in a packed-fluidized bed is not straightforward since the intersection of the two parts in the curve becomes milder.[13] The presence of packing in a bed of a certain height can be expected to decrease the pressure drop, compared to a bed with no packing.[13] This behavior can be attributed to the reduced amount of fluidized particles in the bed due to the presence of the packings. In contrast, if the pressure drop per mass of particles is considered, it will become higher in a packed-fluidized bed due to the additional hindering effect of packings.[25,41] Thus, the type of packings could affect the pressure drop in packed-fluidized beds highly significantly.[41] At gas velocities relevant for bubbling fluidized beds, the pressure drop over a bed containing only the packing material and no fluidizing bed material is negligible. Thus, any deviation of pressure drop for a given mass of particles in a packed-fluidized bed, compared to the case with no packing, can be attributed to the packing−particle interaction. The contribution of spherical packings on pressure drop and similar phenomena such as bed expansion has been studied in the literature,[24,29] where the general effects of packings on pressure drop in confined fluidization described above have been established. Thus, by knowing the mass of particles presented in a given packed volume, the total pressure drop per mass of fluidized particles can be estimated.

In this work, both the pressure drop for a given bed height and the pressure drop for a given particle bed mass were investigated. The aim was to evaluate how the pressure drop was affected by the packing−particle interaction. Also, the pressure drop of the segregated section over the packing material region was measured. This was done with a pressure sensor located at the height where the packed region ended, i.e., 13 cm above the gas distributor plate.

3.3. Vertical Segregation in Packed-Fluidized Beds. A bed of stationary packings and fluidizing particles will divide into two distinct regions at sufficiently high superficial gas velocities.[41] The bottom region is made up of packings and fluidized particles. Also, a dense phase of segregated fluidizing solids will accumulate on its top (Figure 5). This top layer shows similar properties as a fluidized bed containing no packing material.

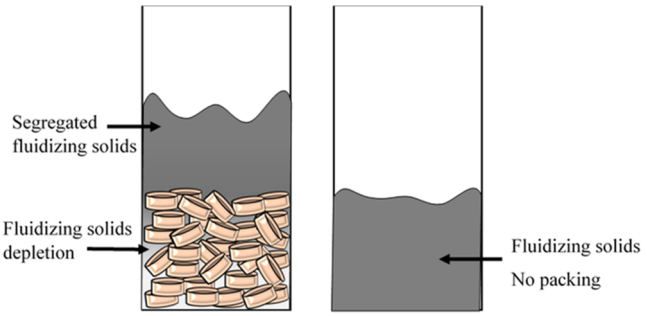

Figure 5. Vertical segregation in packed-fluidized beds at high superficial gas velocities.

By placing a pressure sensor at the height where the packed region ends in the resting state of a reactor (in this study 13 cm above the distributor plate), the pressure drop induced due to the segregation above the packing can be measured. One assumption that needs to be made is that this region will have the same mass of bed material per pressure drop ratio, $m_p/\Delta P$, as a bubbling bed containing no packings and operating at the same conditions with respect to temperature and velocity. Under these assumptions, the mass of fluidizing particulate materials in the region above packings can be estimated as

https://doi.org/10.1021/acs.iecr.1c01221
Ind. Eng. Chem. Res. 2021, 60, 10365−10375

$$m_{p,top} = \Delta P_{top}\left(\frac{m_p}{\Delta P}\right)_{no\ packing} \quad (16)$$

Since the total weight of fluidizing particles introduced into the reactor is known, it is possible to do a mass balance for each situation. It was assumed that there was a negligible loss of bed particles during the experiments from entrainment. No such entrainment was observed, and this should be a sound assumption when using silica sand of this size range at the superficial gas velocities used.

$$m_{p,tot} = m_{p,top} + m_{p,pack} \quad (17)$$

The void fraction of the particles in the packed zone is related to the mass of particles within that specific volume. The relationship between the void fraction and the fluidizing particle mass inside the packed zone can be obtained by eq 18.

$$\varepsilon_{p,packing} = \left(\frac{1-\varepsilon_p}{m_{p,tot}}\right)m_{p,top} + \varepsilon_p \quad (18)$$

where ε_p is the void fraction of particles at rest. Essentially, eq 18 shows the linear relationship between two boundary conditions, namely, when all particles are maintained in the packed zone ($m_{p,top} = 0$ and $\varepsilon_{p,packing} = \varepsilon_p$) and when all particles are located above the packed zone ($m_{p,top} = m_{p,tot}$ and $\varepsilon_{p,packing} = 1$).

4. RESULTS

4.1. Heat Transfer Coefficient. The effect of temperature on the heat transfer coefficient for packed-fluidized beds with different packings is presented in Figure 6. The results showed

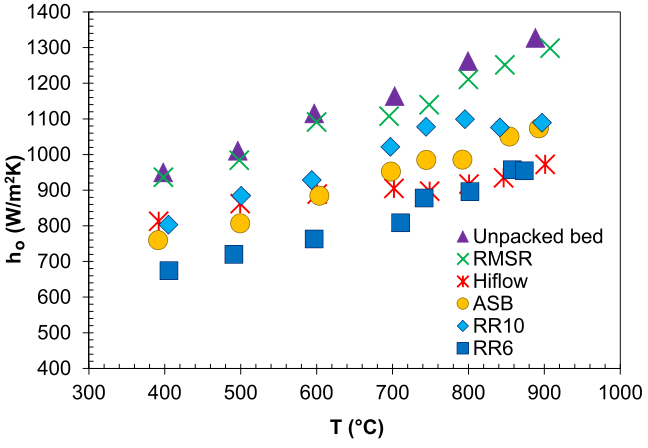

Figure 6. Effect of bed temperature on the heat transfer coefficient for different packings (superficial gas velocity, 0.2 m/s; water flow rate, 20 mL/s; and initial bed and packing height, 13 cm).

that the heat transfer coefficient varied significantly (671−1298 W/m^{2}K) in the tested temperature range of 400−900 °C at a superficial gas velocity of 0.2 m/s.

As can be seen in Figure 6, the bed with no packing showed a higher heat transfer coefficient compared to packed-fluidized beds. Among the packed-fluidized beds, RMSR displayed the highest heat transfer coefficient. It can be observed from Figure 6 that RMSR performed about equal as compared to a bed with no packings. RR10 displayed the second-highest heat transfer coefficients, followed by ASB. Both these packings followed a similar trend with increased heat transfer with increasing bed temperature. Sutherland et al.[13] investigated heat transfer for spherical packings and observed that smaller packings restrict particle movements more and thus decrease heat transfer inside the bed; these observations are in agreement with the results for RR10 and RR6. By decreasing the size of RRs from 10 to 6 mm, bed restriction and channeling could be expected to intensify, which will lower the heat transfer coefficient. Hiflow packings provided somewhat peculiar results. Despite the similar nominal attributes of Hiflow and RMSR with respect to nominal size and void factor, the heat transfer when using Hiflow packing was significantly less good than that for the RMSR packings. This will be discussed in Section 5 below.

Figure 6 also shows that the heat transfer coefficient increased roughly linearly with increasing bed temperature for all packings. This trend agrees with other studies in which conventional fluidized beds were investigated for different temperature ranges and bed materials.[37,42,43] Mathur and Saxena[42] and Grewal and Menart[43] attributed this increase to increasing gas thermal conductivity and increasing bubble phase and emulsion phase radiative fluxes. Stenberg et al.[37] also observed that by increasing the temperature from 400 to 950 °C in a bubbling fluidized bed with silica sand, ilmenite, and ground steel converter slag as bed materials, the radiative contribution to the overall heat transfer would increase from a few percent at 400 °C up to as much as 15% at 950 °C.

Figure 7 shows the effect of superficial gas velocity on the heat transfer coefficient for different types of packings.

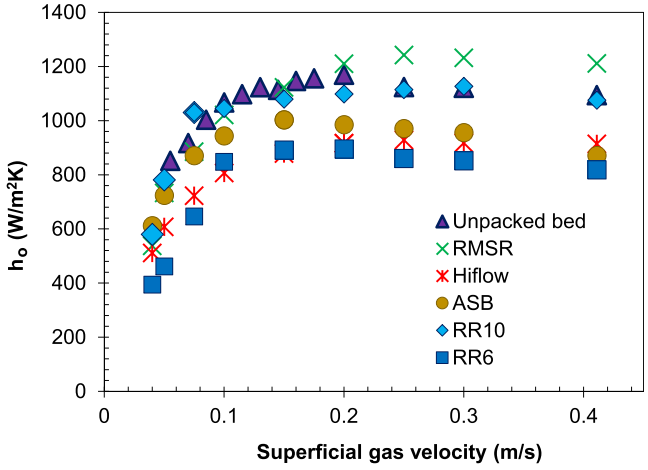

Figure 7. Effect of superficial gas velocity on the heat transfer coefficient for different packings (temperature, 800 °C; water flow rate, 20 mL/s; and unfluidized bed height, 13 cm).

As shown in Figure 7, the heat transfer coefficient increases sharply at lower velocities. Then, after reaching a maximum value, it becomes rather constant or decreases slightly. This agrees well with the results presented in the literature for beds without packings.[37] Figure 7 illustrates that at high superficial gas velocities, packed-fluidized beds with RMSR packings show a higher heat transfer coefficient, 1243 W/m^{2}K, compared to other cases, including the bed without packing, which displayed a maximum heat transfer coefficient of 1124 W/m^{2}K. This feature can possibly be attributed to the ability of packings to break large bubbles into smaller ones. To facilitate understanding, the behavior of a bed with no packing and increasing gas velocity will be considered. The particulate bed

https://doi.org/10.1021/acs.iecr.1c01221
Ind. Eng. Chem. Res. 2021, 60, 10365−10375

can, in this case, be divided into two different phases, the emulsion phase and the bubble phase.[44,45] By increasing gas velocity at a fixed temperature, initially, formation of small bubbles will help in increasing the interaction of bed particles with each other and the surface of the water tube. Thus, it will increase heat transfer between the bed material and tube. However, increasing the gas velocity to higher values will increase the number of bubbles. Eventually, bubble coalescence will occur and result in the formation of bigger bubbles.[14,45] Since heat transfer is a function mainly of particles coming in direct contact with the tube, this will reduce the heat transfer coefficient. A packing with a high void factor, such as RMSR, that does not greatly hinder particle movement but breaks down big bubbles to smaller ones, could therefore conceivably improve the heat transfer coefficient to a submerged tube, as have been observed.

4.2. Pressure Drop. Figure 8 shows the total pressure drop over the bed (from the distributor plate to the atmosphere) as a function of superficial gas velocity.

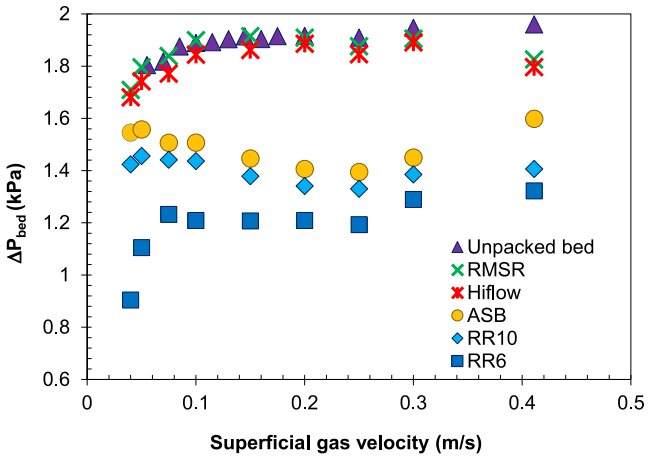

Figure 8. Total pressure drop as a function of superficial gas velocity for different packings (temperature, 800 °C; water flow rate, 20 mL/s; and unfluidized bed height, 13 cm).

The pressure drop was calculated as windbox pressure minus the known pressure drop over the gas distributor plate in an empty reactor for the operating conditions used. There is a weak trend for all packed beds except ASB to exhibit a decrease in pressure drop with increasing superficial gas velocity at some point. This agrees well with other studies investigating the pressure drop in packed-fluidized beds with spherical packings.[13,41] This is likely due to the decreasing amount of bed material present in the packed region with increasing velocity, which is due to an increase in vertical segregation. The pressure drop for ASB also had a decreasing trend at lower velocities but was found to increase at higher velocities. It is worth mentioning that all cases with packings showed a lower pressure drop compared to the case with no packings, which could be expected. The reason for this behavior would be that a smaller mass of fluidized bed material is present in a packed bed, compared to a bed with no packing. The pressure drop per mass of fluidizing bed material as a function of superficial gas velocity is shown in Figure 9.

It can be observed that the pressure drop per mass of particles for RMSR and Hiflow packings is approximately constant and rather close to that of the bed with no packing. It seems clear that these two packings, both of which have a very

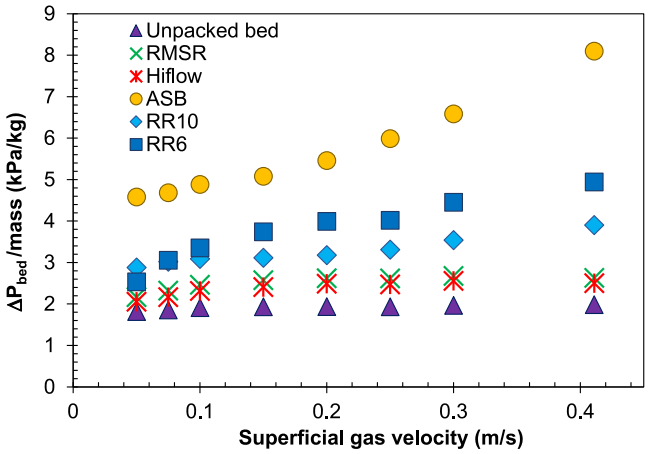

Figure 9. Pressure drop per unit bed mass as a function of superficial gas velocity for different packings (differential pressure between the bottom of the bed and the probe located at 13 cm; temperature, 800 °C; water flow rate, 20 mL/s, and initial bed and packing height, 13 cm).

high void factor of >95%, have lower friction between the particles and packings compared with the other packings. Thus, they behave largely like unpacked beds in this respect. Packings with a lower void factor, such as RRs and especially the ASB packings, display higher pressure drop per mass of bed material. The main reason should be the interaction between fluidization gas, bed particles, and packing material, as was outlined above.

4.3. Vertical Segregation of Fluidizing Solids. The voidage of the fluidizing solids inside different packed beds ($\varepsilon_{p,packing}$), calculated from the differential pressure between the bottom of the bed and the probe located 13 cm above the distributor plate, is illustrated in Figure 10.

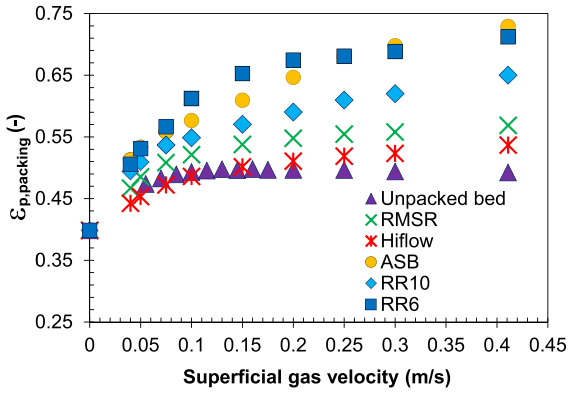

Figure 10. Voidage of fluidizing solids versus superficial gas velocity for different packings (pressure probe at 13 cm above the distributor plate; temperature, 800 °C; water flow rate, 20 mL/s; and initial bed and packing height, 13 cm).

$\varepsilon_{p,packing}$ represents how a large fraction of the fluidized volume from the bottom plate up to the packed height at 13 cm consists of gas. Consequently, $(1 - \varepsilon_{p,packing})$ represents how much of the fluidized bed material is present. The starting point for all cases is the void factor of the bed material with or without packing at rest, i.e., gas velocity equals zero. For approximately spherical sand particles, $\varepsilon_{p,packing} \approx 0.4$ at rest. Figure 9 shows that $\varepsilon_{p,packing}$ increases with superficial gas

https://doi.org/10.1021/acs.iecr.1c01221
Ind. Eng. Chem. Res. 2021, 60, 10365−10375

velocity. For the bed without packing, this represents the expected bed expansion when fluidization is initiated. For the packed beds, in addition to ordinary bed expansion, it can be expected that some bed material is moved from the voids inside the packed zone to the space above them and is prohibited from falling back into the bed. Figure 10 shows that the $\varepsilon_{p,packing}$ for Hiflow and RMSR packings is lower than that for other packed beds and rather close to that of the bed with no packings. This shows that Hiflow and RMSR packings were much better in retaining the bed material in the packed zone up to 13 cm reactor height than the other packings, which suffered from larger tendencies toward extensive vertical segregation at higher gas velocities. Thus, it can be concluded that to avoid excessive bed material segregation, packings with high void factors are preferred.

5. DISCUSSION

Generally, if compared to a common bubbling fluidized bed, packings with a low void factor such as RR6 (void factor, 0.50), RR10 (void factor, 0.58), and ASB (void factor, 0.43) showed (i) reduced heat transfer coefficient (Figures 6 and 7), (ii) lower pressure drop over the bed as a whole (Figure 8), (iii) higher pressure drop per mass of fluidized particles in the bed (Figure 9), and (iv) much more pronounced vertical segregation (Figure 10) compared to a bed without packings. With respect to heat transfer, packings of this type will cover parts of the outer surface of the horizontal tube and decrease the efficient surface area for direct particle-to-tube heat transfer. Also, packings will, to a certain extent, hinder the freedom of movement for particles, which could potentially decrease heat and mass transfer within the bed itself, as well as to the pipe. As for vertical segregation, packings with a low void factor (RR6, RR10, and ASB) will increase the actual gas velocity in the packed zone and may also propagate channeling.

In contrast, packings with a high void factor such as RMSR and Hiflow displayed behavior more similar to a bed without packings, which is not unexpected. When using this sort of packings, more than 95% of the reactor volume is still fluidized particles. The single observation, which is counterintuitive, is the relatively poor heat transfer to the tube when using Hiflow packings. Key results and implications for possible applications for packed-fluidized beds will be discussed below.

5.1. Potential Sources of Error. One hypothesis is that packings, especially packings with low voidage, could intensify tendencies toward channeling along the walls and in immediate connection to the pipe and that this could result in reduced heat transfer and increased vertical segregation. To investigate this phenomenon, a set of experiments were carried out at room temperature in a cylindrical cold flow model made of Plexiglas with an inner diameter of 12 cm and a height of 1 m. The gas velocities were in the range of 0.02−1 m/s. Initial bed and packing heights for these experiments were set at 12 and 24 cm, respectively. Channeling was initiated already at gas velocities of 0.07−0.1 m/s in the bed containing RRs. Figure 11 shows the channeling of silica sand particles with an average diameter of 240 μm in a bed containing RR10 and ASB packings. For these types of packings, significant amounts of sand particles were also displaced to the zone above packings and tended to form a segregated section there.

A similar set of experiments were done with Hiflow packings and RMSR packings. Observations showed that for both these packings, channeling was much less probable to take place

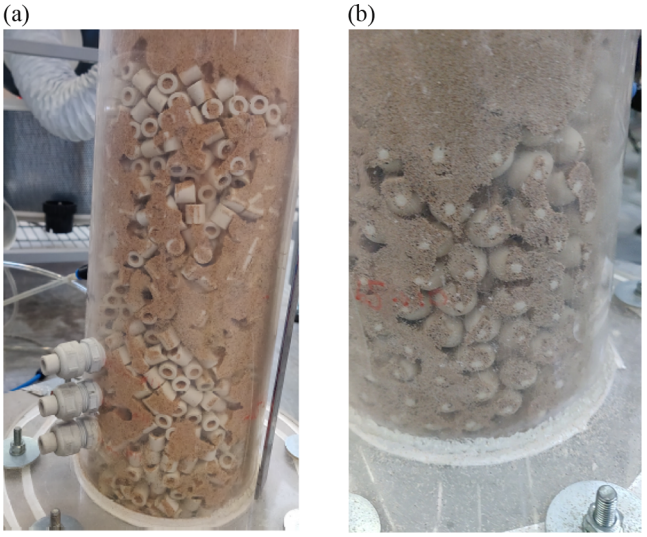

Figure 11. Channeling for (a) RR10 and (b) ASB in a bed of silica sand particles with a mean diameter of 240 μm, bulk density of 1594 kg/m^3, superficial gas velocity in the range of 0.35−1 m/s, and an initial bed height of 12 cm.

compared to low void packings, even at high gas velocities. Sand particles appeared to move freely and largely stayed in the packing zone, as shown in Figure 12.

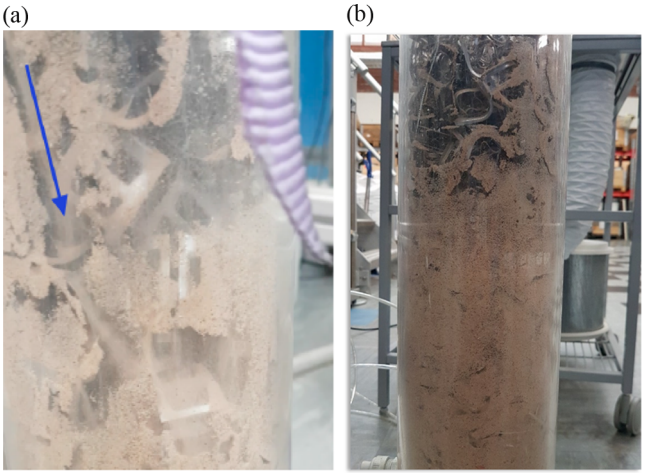

Figure 12. Experiments with (a) Hiflow packings and (b) RMSR packings in a bed of silica sand particles with a mean diameter of 240 μm, bulk density of 1594 kg/m^3, superficial gas velocity in the range of 0.35−1 m/s, and an initial bed height of 12 cm.

In Figure 12a, it can be seen that for Hiflow packings, some channelings could be observed at high gas velocities (around 0.7 m/s at room temperature), especially near the wall. This is a relevant observation. The impact of the reactor walls when using comparably large packings in experimental reactors of the size used could be highly significant. RMSR and Hiflow both have a nominal size of 25 mm. Still, they represent the smallest commercial packings of their types, which we found to be available. For the stainless steel reactor, which had a diameter of 77.9 mm, the wall effects could possibly be more severe.

While RMSR and Hiflow nominally are of the same size, Hiflow clearly is much bulkier and packs less readily in the small reactors used (see Figure 2). It is conceivable that this could be the reason behind the unexpectedly poor heat transfer

https://doi.org/10.1021/acs.iecr.1c01221
Ind. Eng. Chem. Res. 2021, 60, 10365−10375

coefficient to the tube for Hiflow packings. For example, if much gas passes through channeling near the walls, there would be less particle mobility near the tube. Thus, the relatively small diameter of the reactor vessel as compared to the packing size may have been a shortcoming of the study, as it could be susceptible to wall effects such as channeling.

Another potential source of error is related to the water tube temperature measurements. This possibility has been investigated in detail in another work utilizing the same general reactor setup as used in this study.[37] The temperature on the water outlet side is measured 2 cm from the wall. However, the impact of the measurement point chosen was shown to be so low that it could be neglected.[37] In the same study, it was also shown that the heat transfer due to conduction between the connection point of the water tube to the reactor wall and the stagnant air environment inside the furnace was negligible.[37] The contribution from stagnant air in convective and radiative heat transfer in comparison to the efficient heat transfer due to fluidization was also found to be small and negligible.[37] Another possible source of error is the effect of conduction between the reactor wall and the water tube. However, the reactor wall close to the water tube was found to be cooled by the cold water flow.[37]

6. CONCLUSIONS

In this work, the effect on some key performance indicators for choosing different packings in a packed-fluidized bed reactor operating at elevated temperatures was examined. The void factor is identified as a key characteristic of the packings. RMSR and Hiflow are characterized by their high void factor (>95%), while RR10, RR6, and ASB have a much lower void factor (<58%). The following conclusions are drawn:

- All packed-fluidized bed configurations resulted in a lower heat transfer coefficient to a submerged tube than that of a bed containing no packing, at the superficial gas velocity of 0.2 m/s and bed temperatures corresponding to 400−900 °C. However, the impact of RMSR was almost negligible.
- When increasing the superficial gas velocity at the fixed temperature of 800 °C, the heat transfer coefficient in packed beds containing RMSR packings eventually became higher than that for the bed without packings. This is attributed to the ability of the packings to prevent formation of large bubbles inside the bed, while not significantly hindering the mobility of fluidized particles.
- The pressure drop for a given bed height decreases for all packings compared to a bed without packings. This is likely due to a lower mass of fluidized particles being present in the given volume due to the space occupied by the stagnant packing.
- The pressure drop expressed per mass of fluidized particles is affected by the packing. For RMSR and Hiflow packings, the pressure drop per mass of fluidized particles is quite close to those of beds containing no packings (about 20% increase). For RR6, RR10, and especially ASB, the increase is 60−400%, depending on packing and gas velocity. Thus, it is clear that packings with low void factors induce significant friction to the system. This is likely an effect of high local gas velocities.
- Packings with high void factors were found to induce only limited vertical segregation of the bed material. Conversely, the packings with low void factors, RR6, RR10, and ASB, induced noticeable segregation of the bed material, especially at high gas velocities.

The results indicate that packings with a high void factor, with RMSR being the best example, could be added to a bubbling fluidized bed with limited effect on heat transfer, pressure drop, and vertical segregation. This is a significant finding since the ability of packings to reduce bubble size and improve gas−solid mass transfer could be expected to be significant. Packings with a low void factor, with ASB being the best example, have a much higher impact on fluidization in general. There may be other uses for this kind of packing in fluidized beds, although they remain to be discovered.

AUTHOR INFORMATION

Corresponding Author

Nasrin Nemati − *Division of Energy Technology, Department of Space, Earth and Environment, Chalmers University of Technology, Göteborg 412 96, Sweden;* orcid.org/0000-0001-7860-2034; Email: nasrinn@chalmers.se

Authors

Pontus Andersson − *Division of Energy Technology, Department of Space, Earth and Environment, Chalmers University of Technology, Göteborg 412 96, Sweden*

Viktor Stenberg − *Division of Energy Technology, Department of Space, Earth and Environment, Chalmers University of Technology, Göteborg 412 96, Sweden*

Magnus Rydén − *Division of Energy Technology, Department of Space, Earth and Environment, Chalmers University of Technology, Göteborg 412 96, Sweden*

Complete contact information is available at: https://pubs.acs.org/10.1021/acs.iecr.1c01221

Notes

The authors declare no competing financial interest.

ACKNOWLEDGMENTS

This work has been supported by the Swedish Energy Agency (project 46525-1-The application of confined fluidization in energy conversion). The authors also like to acknowledge inputs from the BSc project of Julia Cramstedt, Jesper Larsson, Max Wassenius, and Mårten Bengtsson performed at Chalmers University of Technology (project SEEX15-20-1-Packed fluidized bed fluidization properties).

NOMENCLATURE

A_i	tube inner surface area (m^2)
A_o	tube outer surface area (m^2)
ASB	aluminum silicate ball
$C_{p,water}$	heat capacity of water (J/kgK)
d_i	inner tube diameter (m)
d_o	outer tube diameter (m)
dp	particle diameter (m)
g	acceleration of gravity (9.8 m/s^2)
g_c	conversion factor (1 kg.m/Ns^2)
H	height of the fluidized bed (m)
h_i	heat transfer coefficient from the tube wall to water flow (W/m^2K)
h_o	heat transfer coefficient from the bed to tube (W/m^2K)
Hiflow 25-5	Hiflow
j_H	tube inside heat transfer factor (−)

https://doi.org/10.1021/acs.iecr.1c01221
Ind. Eng. Chem. Res. 2021, 60, 10365−10375

k_{wall}	tube wall thermal conductivity (W/mK)
k_{water}	water thermal conductivity (W/mK)
$m_{p,pack}$	mass of bed particles in the packing region (kg)
$m_{p,top}$	mass of bed particles in the top region (kg)
$m_{p,tot}$	total mass of bed particles (kg)
Pr	Prandtl number (−)
Q	heat transferred through the tube wall (W)
Re	Reynolds number (−)
RMSR	RMSR 25-3
RR6	Raschig ring 6 mm
RR10	Raschig ring 10 mm
T_{bed}	bed temperature (K)
$T_{wall,avg}$	average temperature of the wall (K)
$T_{wall,in}$	temperature of the inside of the tube wall (K)
$T_{wall,out}$	temperature of the outside of the tube wall (K)
$T_{water,avg}$	average water temperature inside the tube (K)
$T_{water,inlet}$	inlet water temperature (K)
$T_{water,outlet}$	outlet water temperature (K)
u_{mf}	superficial gas velocity at minimum fluidization conditions (m/s)
U_o	overall heat transfer coefficient (W/m^2K)
u_{water}	water velocity inside the tube (m/s)
V	water flow rate (m^3/s)

GREEK LETTERS

ΔP_{bed}	pressure drop over the fluidized bed (Pa)
ΔP_{top}	pressure drop over the top region of the bed (Pa)
ΔT_{LM}	logarithmic mean temperature (K)
ΔT_{in}	inlet side temperature difference (K)
ΔT_{out}	outlet side temperature difference (K)
ε_{bed}	void fraction of fluidized bed (−)
ε_p	fixed bed void fraction of bed particles (−)
$\varepsilon_{p,packing}$	packing volume void fraction (−)
μ_g	dynamic viscosity of fluidizing gas (kg/ms)
ρ_s	density of fluidizing bed material (kg/m^3)
ρ_g	density of fluidizing gas (kg/m^3)
ρ_{water}	density of water (kg/m^3)

REFERENCES

(1) Daizo, K.; Levenspiel, O. *Fluidization Engineering*, 2nd ed.; Butterworth-Heinemann: Stoneham, Massachusetts, USA, 1991.

(2) Johnsson, J. E.; Grace, J. R.; Graham, J. J. Fluidized-Bed Reactor Model Vwrification on a Reactor of Industrial Scale. *AIChE J.* **1987**, *33*, 619−627.

(3) Uraz, C.; Atalay, S. Oxidation of Benzene to Maleic Anhydride in a Fluidized Bed Reactor. *Chem. Eng. Technol.* **2007**, *30*, 1708−1715.

(4) Westerink, E. J.; Westerterp, K. R. Stable Design and Operation of Catalytic Fluidized-Bed Reactors for Multiple Reactions: Uniqueness and Multiplicity. *Chem. Eng. Sci.* **1990**, *45*, 317−332.

(5) Leckner, B. Fluidized Bed Reactors: Heat and Mass Transfer. In *Multiphase Flow Handbook*, Michaelides, C. T.; Crowe, J. D., Eds.; CRC Press, 2017; pp 994−1029.

(6) Flamant, G.; Fatah, N.; Flitris, Y. Wall-to-Bed Heat Transfer in Gas-Solid Fluidized Beds: Prediction of Heat Transfer Regimes. *Powder Technol.* **1992**, *69*, 223−230.

(7) Grewal, N. S.; Saxena, S. C. Heat Transfer Between a Horizontal Tube and a Gas-Solid Fluidized-Bed. *Int. J. Heat Mass Transfer* **1980**, *23*, 1505−1519.

(8) Andeen, B. R.; Glicksman, L. R. *Heat Transfer to Horisontal Tubes in Shallow Fluidized Beds*. ASME-AIChe Heat Transfer Conference, St Louis, MO, 1976.

(9) Genetti, W. E.; Schmall, R. A.; Grimmett, E. S. The Effect of Tube Orientation on Heat Transfer with Bare and Finned Tubes in a Fluidized Bed. *Chem. Engr. Progr. Sym. Ser.* **1971**, *116*, 90−96.

(10) Gelperin, N. I.; et al. Heat Transfer Between a Fluidized Bed and a Surface. *Int. Chem. Eng.* **1966**, *6*, No. 67.

(11) Vreedenberg, H. A. Heat Transfer Between a Fluidized Bed and a Horizontal Tube. *Chem. Eng. Sci.* **1958**, *9*, 52−60.

(12) Stenberg, V.; Lind, F.; Rydén, M. Measurement of bed-to-tube surface heat transfer coefficient to a vertically immersed u-tube in bubbling loop seal of a CFB boiler. *Powder Technol.* **2021**, *381*, 652−664.

(13) Sutherland, J. P.; Vassilatos, G.; Kubota, H.; Osberg, G. L. The effect of packing on a fluidized bed. *AIChE J.* **1963**, *9*, 437−441.

(14) Geldart, D. Types of Gas Fluidization. *Powder Technol.* **1973**, *7*, 285−292.

(15) Grace, J. R. Contacting Modes and Behaviour Classification of Gas-Solid and Other Two-Phase Suspensions. *Can. J. Chem. Eng.* **1986**, *64*, 353−363.

(16) Schmitz, M.; Linderholm, C. Chemical Looping Combustion of Biomass in 10- and 100-kW Pilots-Analysis of Conversion and Lifetime Using a Sintered Manganese Ore. *Fuel* **2018**, *231*, 73−84.

(17) Radmanesh, R.; Chaouki, J.; et al. *Biomass Gasification in a Bubbling Fluidized Bed* Reactor: Experiments and Modeling. *AIChE J.* **2006**, *52*, 4258−4272.

(18) Wang, Y.; et al. A New Drag Model for TFM Simulation of Gas-Solid Bubbling Fluidized Beds With Geldart-B Particles. *Particuology* **2014**, *15*, 151−159.

(19) Wang, H.; et al. Study of Bubbling and Slugging Fluidization Beds by Simulation and ECT. *AIChE J.* **2006**, *52*, 3078−3087.

(20) Hosseini, S. H.; et al. CFD Simulation of the Bubbling and Slugging Gas-Solid Fluidized Beds. *ASME. J. Fluids Eng.* **2010**, *132*, No. 041301.

(21) Ma, J.; et al. Fluidization dynamics of cohesive Geldart B particles. Part I: X-ray tomography analysis. *Chem. Eng. J.* **2019**, *359*, 1024−1034.

(22) Shaul, S.; Rabinovich, E.; Kalman, H. Typical Fluidization Characteristics for Geldart's Classification Groups. *Part. Sci. Technol.* **2014**, *32*, 197−205.

(23) Song, X.; et al. Gas-Solids Circulating Fluidization in a Packed Bed. *Powder Technol.* **1995**, *83*, 127−131.

(24) Donsì, G.; Ferrari, G.; Formisani, B.; Longo, G. Confined Fluidization of Fine Particles in a Packed Bed of Coarse Particles: Model and Experimental Description. *Powder Technol.* **1990**, *61*, 75−85.

(25) Donsì, G.; Ferrari, G.; Formisani, B. Expansion behaviour of confined fluidized beds of fine particles. *Can. J. Chem. Eng.* **1989**, *67*, 185−190.

(26) Girimonte, R.; Vivacqua, V. The Expansion Process of Particle Beds Fluidized in The Voids of a Packing of Coarse Spheres. *Powder Technol.* **2011**, *213*, 63−69.

(27) Girimonte, R.; Vivacqua, V.; Formisani, B. Extension of the Model of Binary Fluidization to Beds Confined in a Packing of Coarse Spheres. *Powder Technol.* **2016**, *297*, 275−282.

(28) Girimonte, R. F. B.; Testa, F. CO2 Adsorption in a Confined Fluidized Bed of Zeolite Pellets: Influence of Operating Velocity. *Particuology* **2019**, *46*, 67−74.

(29) Girimonte, R.; Formisani, B.; Testa, F. Adsorption of CO2 on a Confined Fluidized Bed of Pelletized 13X Zeolite. *Powder Technol.* **2017**, *311*, 9−17.

(30) Mandal, D.; Vinjamur, M.; Sathiyamoorthy, D. Hydrodynamics of beds of small particles in the voids of coarse particles. *Powder Technol.* **2013**, *235*, 256−262.

(31) Mandal, D.; Sathiyamoorthy, D.; Vinjamur, M. Experimental investigation of heat transfer in gas−solid packed fluidized bed. *Powder Technol.* **2013**, *246*, 252−268.

(32) Mandal, D.; Sathiyamoorthy, D.; Vinjamur, M. Void fraction and effective thermal conductivity of binary particulate bed. *Fusion Eng. Des.* **2013**, *88*, 216−225.

(33) Mandal, D.; Sathiyamoorthy, D.; Vinjamur, M. Heat Transfer Characteristics of Lithium Titanate Particles in Gas-Solid Packed Fluidized Beds. *Fusion Sci. Technol.* **2012**, *62*, 150−156.

https://doi.org/10.1021/acs.iecr.1c01221
Ind. Eng. Chem. Res. 2021, 60, 10365−10375

(34) Mandal, D. Hydrodynamics of particles in liquid−solid packed fluidized bed. *Powder Technol.* **2015**, *276*, 18−25.
(35) Mandal, D.; et al. Quality of fluidization in gas−solid unary and packed fluidized beds: An experimental study using gamma ray transmission technique. *Powder Technol.* **2012**, *226*, 91−98.
(36) Kulkarni, N. J.; Mathpati, C. S.; Mandal, D.; Dalvi, V. H. Minimum Fluidization Velocity of Intermediate Sized Particles in Conventional and Packed Fluidized Bed. *Int. J. Chem. React. Eng.* **2019**, *17*, 20180321.
(37) Stenberg, V.; Sköldberg, V.; Öhrby, L.; Rydén, M. Evaluation of bed-to-tube surface heat transfer coefficient for a horizontal tube in bubbling fluidized bed at high temperature. *Powder Technol.* **2019**, *352*, 488−500.
(38) Welty, J.; Wicks, C.; Wilson, R.; Rorrer, G. *Fundamentals of Momentum, Heat and Mass Transfer*; Wiley: Hoboken, N.J., USA, 2005.
(39) Incropera, F.; D, D.; Bergman, T.; Lavine, A. *Principles of Heat and Mass Transfer*; Singapore, 2013.
(40) Sinnott, R. K.; Coulson, J. M.; Richardson, J. F. *Coulson & Richardson's Chemical Engineering*, 2005; Vol. *6*.
(41) Aronsson, J.; Pallarès, D.; Rydén, M.; Lyngfelt, A. Increasing Gas−Solids Mass Transfer in Fluidized Beds by Application of Confined Fluidization—A Feasibility Study. *Appl. Sci.* **2019**, *9*, No. 634.
(42) Mathur, A.; Saxena, S. C. Total and Radiative Heat Transfer to an Immersed Surface in a Gas- Fluidized Bed. *AIChE J.* **1987**, *33*, 1124−1135.
(43) Grewal, N. S.; Menart, J.; et al. Heat Transfer to Horizontal Tubes Immersed in a Fluidized-Bed Combustor. *Powder Technol.* **1987**, *52*, 149−159.
(44) Rhodes, M. *Introduction to Particle Technology*; John Wiley & Sons Ltd, England, 2008.
(45) Nemati, N.; Zarghami, R.; Mostoufi, N. Investigating the Hydrodynamics of High Temperature Fluidized Beds by Pressure Fluctuations. *Chem. Eng. Technol.* **2016**, *39*, 1527−1536.

https://doi.org/10.1021/acs.iecr.1c01221
Ind. Eng. Chem. Res. 2021, 60, 10365−10375